Realization of a large J_2 quasi-2D spin-half Heisenberg system: Li_2VOSiO_4

H. Rosner*,[1], R.R.P. Singh[1], W.H. Zheng[2], J. Oitmaa[2], S.-L. Drechsler[3], and W.E. Pickett[1]
[1] *Department of Physics, University of California, Davis, CA 95616, USA*
[2] *School of Physics, University of New South Wales, Sydney NSW 2052, Australia*
[3] *Institut für Festkörper- und Werkstofforschung Dresden e.V., Postfach 270116, D-01171 Dresden, Germany*
(November 20, 2001)

Exchange couplings are calculated for Li_2VOSiO_4 using LDA. While the sum of in-plane couplings $J_1 + J_2 = 9.5 \pm 1.5$K and the inter-plane coupling $J_\perp \sim 0.2$–0.3K agree with recent experimental data, the ratio $J_2/J_1 \sim 12$ exceeds the reported value by an order of magnitude. Using geometrical considerations, high temperature expansions and perturbative mean field theory, we show that the LDA derived exchange constants lead to a remarkably accurate description of the properties of these materials including specific heat, susceptibility, Neél temperature and NMR spectra.

71.15.Mb,75.10.Jm,75.30.Et

In many recently discovered magnetic materials the determination of exchange constants, without input from electronic structure calculations, has proven very difficult and has often led to wildly incorrect parameter values. The interplay of geometry and quantum chemistry has yielded many surprises which could not have been anticipated without a full calculation. Examples are the recently discovered vanadates CaV_4O_9 [1] and CaV_3O_7 [2]. In all these cases the dominant exchange interactions were resolved and a good understanding of the material properties obtained only after analyses of electronic structure calculations were carried out.

Frustrated square-lattice spin-half Heisenberg antiferromagnets with nearest neighbor exchange J_1 and second neighbor (diagonal) exchange J_2 have received considerable attention recently. The properties of the model with J_2=0 (or J_1=0) are well understood at zero and finite temperature [3]. The large J_2 limit of the model is a classic example of quantum order by disorder [4,5], where at the classical level the two sublattices order antiferromagnetically but remain free to rotate with respect to each other. This degeneracy is lifted by quantum fluctuations leading to collinear magnetic order in a columnar pattern. At intermediate J_2/J_1 there is strong evidence for a spin-gap phase, though the nature of this phase is not fully resolved yet [6].

While there has been tremendous theoretical interest in these models, there were no known experimental realizations for intermediate to large J_2/J_1, until the investigation of Li_2VOSiO_4 by Melzi *et al.* [7,8] Studying the splitting patterns of the ^{7}Li NMR spectra, these authors presented strong evidence for columnar order [7]. Combining several experiments they derive [8] exchange couplings (with $J_2/J_1 \sim 1.1$) well into the region where model calculations find columnar order.

However, several puzzling pieces in that excellent and detailed study remain: (i) The ratio of exchange constants was not well determined from the susceptibility and specific heat data; we will present electronic structure and many-body calculations to show that the J_2/J_1 value is even much larger than reported [8], placing the system deeper into the columnar phase. (ii) The estimated $T = 0$ moment was anomalously small for a system well inside the columnar ordered phase. Taking into account the antiferromagnetic inter-plane coupling, we propose that the NMR derived moment is small due to a cancellation of hyperfine fields from neighboring planes. (iii) The order parameter exponent β at the transition was estimated to be $\beta \approx 0.25$, which is intermediate between 2D Ising and typical 3D exponents. We will show that the inter-plane exchange constants differ from the largest ones by less than two orders of magnitude. Thus a strong crossover between 2D and 3D behavior could be expected. (iv) The Neél temperature was nearly field independent up to a field of $9T$. We will argue that our increased estimate of J_2 leads to a larger saturation field and that combined with non-monotonic dependence of Neél temperature on field implies that the experimental results are not anomalous.

Our study of the material Li_2VOSiO_4 consists of a two band tight-binding model fit to the LDA band structure, which is then mapped onto a Heisenberg model with in-plane (J_1 and J_2) and inter-plane ($J_\perp$) exchange constants. Furthermore, we develop high temperature series expansions and perturbative mean-field theory for the uniform susceptibility and specific heat of the $J_1 - J_2$ model. These allow us to make quantitative comparisons with the experiments.

Li_2VOSiO_4 crystallizes in the tetragonal system, space group $P4/nmm$, containing two formula units per cell with $a = 6.3682$ Å and $c = 4.449$ Å. [9] The crystal structure of Li_2VOSiO_4 is shown in Fig. 1. The magnetically active network of spin half V^{4+} ions is built up by $[VOSiO_4]^{2-}$ layers of VO_5 square pyramids sharing corners with SiO_4 tetrahedra, intercalated with Li ions. The structure of the V^{4+} square network suggests, that both the nearest neighbor (NN) and the next nearest neighbor (NNN) in-plane coupling should be significant, although it is at best difficult to decide from general considerations which one is dominant. NN coupling is favored by the existence of two exchange channels and shorter distance, NNN coupling profits from the 'straight' connection be-

tween pyramids pointing in the same direction.

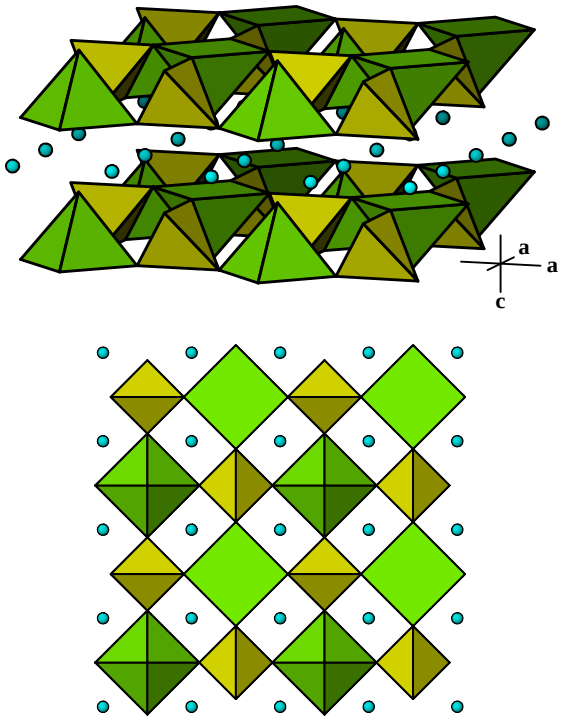

FIG. 1. Perspective view (upper panel) of the crystal structure of Li_2VOSiO_4 and projection along [001] (lower panel). The VO_5 pyramids (large diamonds) share the corners of the basal planes with SiO_4 tetrahedra (small diamonds). The Li^+ ions are indicated by circles.

In order to obtain a realistic and reliable hopping part of a tight-binding Hamiltonian, band structure calculations were performed using the full-potential nonorthogonal local-orbital minimum-basis scheme [10] within the local density approximation (LDA). In the scalar relativistic calculations we used the exchange and correlation potential of Perdew and Zunger [11]. V($3s$,$3p$,$4s$, $4p$, $3d$), O($2s$, $2p$, $3d$), Li($2s$, $2p$) and Si($3s$, $3p$, $3d$) states, respectively, were chosen as the basis set. All lower lying states were treated as core states. The inclusion of V ($3s$,$3p$) states in the valence states was necessary to account for non-negligible core-core overlaps. The O and Si $3d$ as well as the Li $2p$ states were taken into account to increase the completeness of the basis set. The spatial extension of the basis orbitals, controlled by a confining potential [12] $(r/r_0)^4$, was optimized to minimize the total energy.

The results of the paramagnetic calculation (see Fig. 2) show a valence band complex of about 10 eV width with two bands crossing the Fermi level. These two bands, due to the two V per cell, are well separated by a gap of about 3 eV from the rest of the valence band complex and show mainly V $3d_{xy}$ and minor O(2) $2p_{x,y}$ character (oxygens of the basal plane of the VO_5 pyramid) in the analysis of the corresponding orbital-resolved partial densities of states (not shown). The valence bands below the gap and above the Fermi level have almost pure oxygen and vanadium character, respectively. The contribution of Li and Si states is negligible in the energy region shown.

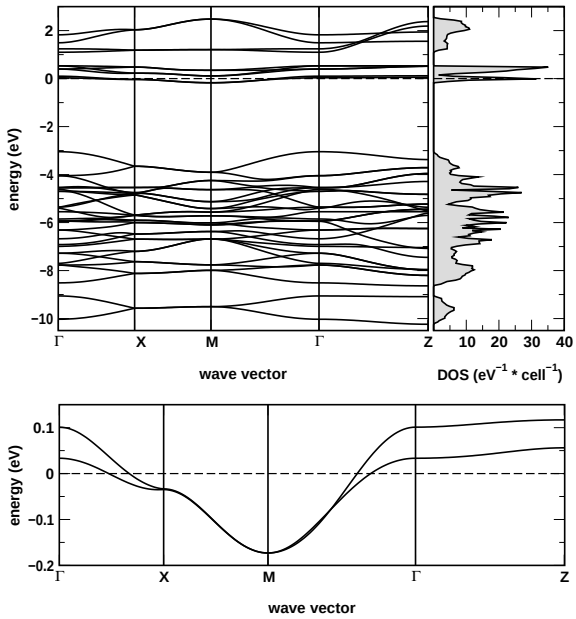

FIG. 2. Band structure and total density of states for Li_2VOSiO_4 (upper panel) and the zoomed bands closest to the Fermi level (lower panel). The Fermi level is at zero energy. The notation of the symmetry points is as follows: X = (100), M = (110), Z = (001)

The relatively narrow bands at the Fermi level (see Fig. 2, lower panel) are half-filled. Therefore, strong correlation effects can be expected which explain the experimentally observed insulating ground state. Because the low-lying magnetic excitations involve only those orbitals with unpaired spins corresponding to the half-filled bands, we restrict ourselves to a two band tight-binding analysis and the discussion of these half-filled bands.

The dispersion of these bands (see Fig. 2, lower panel) has been analyzed in terms of NN transfer t_1 and NNN transfer t_2 within the [001] plane (see Fig. 1 lower panel) and NN hopping $t_\perp$ between neighboring planes.

Then, the corresponding dispersion relation of the related 2×2 problem takes the form

$$E(\vec{k}) = \varepsilon_0 + 2t_2[\cos(x) + \cos(y)] \pm 4t_1 \cos(x/2)\cos(y/2) + 2t_\perp \cos(z)\,, \qquad (1)$$

where $x = k_z a$, $y = k_y b$, $z = k_z c$.

The assignment of the parameters has been achieved by two numerically independent procedures: By straightforward least square fitting of the two bands in all directions and by using the energy eigenvalues at different selected high symmetry points. The results are shown in Table I. The errors can be estimated about 5% for the in-plane transfers and 15% for the inter-plane term

from the differences of both mentioned above fitting procedures. These small differences can be ascribed to the influence of higher neighbors. The very good agreement of the tight binding fit with the LDA bands justifies *a posteriori* the restriction to NN and NNN couplings only.

t_1 (meV)	t_2 (meV)	$t_\perp$ (meV)	U (eV)	J_1 (K)	J_2 (K)	$J_\perp$(K)
8.5	29.1	-4.8	4	0.83	9.81	0.27
			5	0.67	7.85	0.22

TABLE I. Transfer integrals of the two-band tight-binding model and the corresponding exchange couplings for different values of the Hubbard U.

The resulting transfer integrals enable us to estimate the relevant exchange couplings [13], crucial for the derivation and examination of magnetic model Hamiltonians of the spin-1/2 Heisenberg type:

$$H_{spin} = \sum_{ij} J_{ij} \vec{S}_i \cdot \vec{S}_j \,. \qquad (2)$$

In general, the total exchange J can be divided into an antiferromagnetic and a ferromagnetic contribution $J = J^{AFM} + J^{FM}$. In the strongly correlated limit, valid for typical vanadates, the former can be calculated in terms of the one-band extended Hubbard model $J_i^{AFM} = 4t_i^2/(U - V_i)$. The index i corresponds to NN and NNN, U is the on-site Coulomb repulsion and V_i is the inter-site Coulomb interaction. Considering the fact that the VO_5 pyramids are not directly connected, but via SiO_4 tetrahedra, ferromagnetic contributions J^{FM} are expected to be small. For the same reason, the inter-site Coulomb interactions V_i should be small compared with the on-site repulsion U. From LDA-DMFT(QMC) studies [14] and by fitting spectroscopic data to model calculations [15], $U \sim$ 4–5 eV is estimated for typical vanadates. Therefore, we adopt U=4 eV and U=5 eV as representative values to estimate the exchange constants and their sensitivity to U. The calculated values for the exchange integrals are given in Table I.

Comparing our calculated exchange couplings with the experimental findings [8], we find excellent agreement for the sum $J_1 + J_2 = 9.5 \pm 1.5$ K [16] of the in-plane couplings, reported from susceptibility data [8] to be $J_1 + J_2 = 8.2 \pm 1$ K. In contrast, we find a ratio $J_2/J_1 \sim 12$ which exceeds the experimentally derived ratio in Ref. [8] $J_2/J_1 \sim 1.1 \pm 0.1$ by an order of magnitude.

In order to understand the experiments better, we turn to high temperature expansions for the susceptibility and specific heat of the Heisenberg models. Using series expansions (T=0) [17], non-linear sigma model theory [3] (very low-T), quantum Monte Carlo (QMC) simulations (low-T) [18] and high temperature expansions(HTE) (high-T) [19], the susceptibility of the nearest-neighbor model ($J_1 = 0$) is known accurately for all T. Letting $J_2 = 1$ and treating J_1 perturbatively, analogous to chain mean-field theories, [20] leads to the expression

$$\chi(J_1, T) = \chi_0(T)[1 - 4J_1\chi_0(T)] \qquad (3)$$

where χ_0 is the susceptibility for the Heisenberg model ($J_1 = 0$). As shown in the inset of Fig. 3, at $T = 0$ for small J_1/J_2, this expression compares very well with the susceptibility calculated from Ising series expansions. [17] Fig. 3 also shows that applying Eq. 3 to the finite-T QMC data for χ_0 leads to susceptibility values which join smoothly with the high-temperature expansion results. Thus, we have accurate calculations for the susceptibility of the model with small J_1/J_2 at all T.

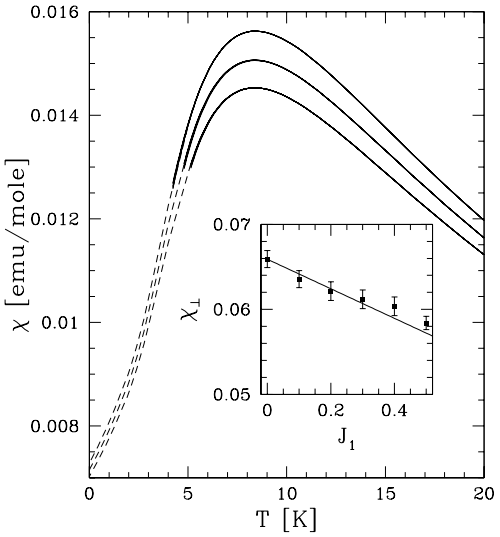

FIG. 3. Susceptibility (χ, with largest χ for $J_1 = 0$) for $J_2 = 9K$, $g = 2$ and $J_1/J_2 = 0, 0.1, 0.2$. The low temperature data is obtained from QMC combined with Eq. 3, while the high temperature data comes from HTE. The inset shows Ising series expansion calculations and Eq. 3 for $T = 0$, $J_2 = 1$.

Rather than find a fit for the exchange constants, in Fig. 3 we show the susceptibility with $g = 2$; $J_2 = 9K$; and $J_1/J_2 = 0, 0.1$ and 0.2. The results are close to experimental values [7]. We note that the agreement will be improved by going to the lower limit of the calculated exchange constants and slightly larger g-values.

The specific heat data was the primary source for the $J_1/J_2 \approx 1$ conclusion by Melzi et al. [8]. They found that the peak value of the specific heat in Li_2VOSiO_4 was $0.436(4)R$ at $T^m = 3.5(1)$. We find that for the pure Heisenberg model the specific heat peaks at $T^m = 0.60(4)J$ with a peak value of $0.455(10)R$, in agreement with Ref. [21]. With small J_1/J_2 the peak shifts to lower temperature and the specific heat becomes flatter. The fact that the values for the pure Heisenberg model are close to the experiments strongly favors a small J_1.

One of the most puzzling aspects of the experimental results [8] is the small moment of 0.24 μ_B at $T = 0$, obtained from the NMR split patterns. In contrast, the moment of the square-lattice Heisenberg model is well

known to be $\approx 0.6\mu_B$. [17] Taking into account the considerable antiferromagnetic inter-plane coupling $J_\perp$ resulting from our calculation, a part of the discrepancy could be understood: The Li nuclei sit between two pairs of inequivalent V-atoms, which results in a partial cancellation of the hyperfine fields from antiferromagnetically ordered NN and NNN V sites (see Fig. 4). This partial cancellation does not change the arguments of Melzi *et al.* for the pattern of line-splitting (including intensities) and its relation to columnar order because the ordering pattern inside the planes remains the same. However, it leads to a reduction in the effective hyperfine coupling and hence to an enhancement of magnetic moment derived from the line shift. Taking into account the calculated two center overlap integrals for Li and NN and NNN V 3d orbitals, respectively, (see Fig. 4) a crude estimate from Slater-Koster integrals suggests that the NMR split would be reduced by an additional factor of about 2. This results in a moment of about 0.5 μ_B much closer to the value expected for the 2D Heisenberg model.

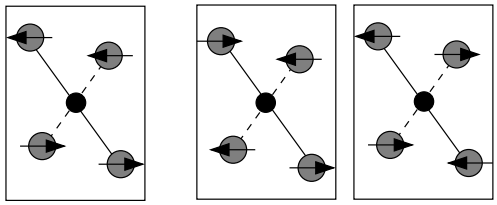

FIG. 4. Sketch of the different magnetic environments for the ^{7}Li NMR. The Li and V sites are represented by black and gray circles, respectively. The arrows indicate the direction of the V spin. Full lines symbolize the stronger interaction with the NN vanadium sites, dashed lines the weaker interaction with the NNN vanadium sites. The different environments cause (a) no NMR shift due to complete moment-cancellation; (b) up or down shift with partial moment-compensation.

We now turn to the inter-plane couplings and the measurements of the Neél temperature, T_N. Applying the expression $T_N \approx 0.36 J_\perp \xi^2(T_N)$ [3] (ξ is the in-plane correlation length), to our calculated exchange constants, leads to the estimate $T_N \approx 3.6 \pm 0.4$ K, which is remarkably close to the experimental value of 2.8 K. Furthermore, the saturation field for our calculated exchange constants is about 30 T, which is much bigger than the 9 T field applied by Melzi *et al.* The Neél temperature should go to zero at the saturation field. However, we note that due to suppression of spin fluctuation the Neél temperature can increase slightly with field, as happens in the purely 2D model. Thus, the experimental result of very weak field dependence of the Neél temperature up to 9 Tesla is consistent with our expectations. The appreciable but still small 3D couplings should also give rise to 3D critical behavior at the finite temperature transition with strong crossover effects. These results on the field dependence of the Neél temperature and the critical behavior at the transition in weakly coupled Heisenberg systems deserve further theoretical attention.

To summarize, we have used LDA to calculate exchange constants for the material Li_2VOSiO_4 and developed numerical studies for the Heisenberg model to show remarkable consistency with many experimental properties. Electronic structure calculations on the closely related material Li_2VOGeO_4 will be presented in a forthcoming publication. The key differences are the considerably smaller J_2/J_1 ratio and coupling to higher neighbors in Li_2VOGeO_4. Finally, we note that both these materials have a substantial 3D coupling, which leads to long-range order at finite T. It would be interesting to find a material with large-J_2 that was nearly 2D, thus closer to exhibiting purely quantum order by disorder.

We thank F. Mila and P. Carretta for discussions. This work was supported by the DAAD (individual grant H.R.), the NSF DMR-9802076 and DMR-9986948, the Deutsche Forschungsgemeinschaft, and by the Australian Research Council.

* Corresponding author: helge@physics.ucdavis.edu

[1] W.E. Pickett, Phys. Rev. Lett. **79**, 1746 (1997).
[2] M.A. Korotin *et al.* Phys. Rev. Lett. **83**, 1387 (1999).
[3] S. Chakravarty, B. I. Halperin and D. R. Nelson, Phys. Rev. Lett. **60**, 1057 (1998).
[4] E. Shender, Sov. Phys. JETP **56**, 178 (1982).
[5] P. Chandra, P. Coleman and A. I. Larkin, Phys. Rev. Lett. **64**, 88 (1990).
[6] O.P. Sushkov, J. Oitmaa and W.H. Zheng, Phys. Rev. B **63** 332 (2001).
[7] R. Melzi *et al.*, Rev. Lett. **85**, 1318 (2000).
[8] R. Melzi *et al.*, Phys. Rev. B **64**, 024409 (2001).
[9] P. Millet and C. Satto, Mat. Res. Bull. bf 33, 1339 (1998).
[10] K. Koepernik and H. Eschrig, Phys. Rev. B **59**, 1743 (1999).
[11] J. P. Perdew and A. Zunger, Phys. Rev. B **23**, 5048 (1981).
[12] H. Eschrig, *Optimized LCAO Method and the Electronic Structure of Extended Systems* (Springer, Berlin, 1989).
[13] H. Rosner *et al.*, Phys. Rev. B **63**, 073104 (2001); M. A. Korotin *et al.*, Phys. Rev. Lett. **83**, 1387 (1999).
[14] K. Held *et al.*, Phys. Rev. Lett. **86**, 5345 (2001).
[15] A. T. Mizokawa, A. Fujimori, Phys. Rev.B **48**, 14150 (1993); J. Zaanen, G. A. Sawatzky, J. Solid State Chem., **88**, 8 (1990).
[16] The specified error results from the uncertainity of U and the errors for t_1 and t_2 from the tight binding fit.
[17] C. J. Hamer, W.H. Zheng, and J. Oitmaa, Phys. Rev. B**50**, 6877 (1994).
[18] J. Kim and M. Troyer, Phys. Rev. Lett. **80**, 2705 (1998).
[19] N. Elstner *et al.*, Phys. Rev. Lett. **75**, 938 (1995).
[20] D. J. Scalapino, Y. Imry, and P. Pincus, Phys. Rev. B **11**, 2042 (1975).
[21] M.S. Makivić and H.-Q. Ding, Phys. Rev. B **43**, 3562 (1991)